Geomechanics and Engineering, *Vol. 26, No. 2 (2021) 161-173*
https://doi.org/10.12989/gae.2021.26.2.161

Allowable wall deflection of braced excavation adjacent to pile-supported buildings

Linlong Mu[1,2], Maosong Huang[1,2], Gholam H. Roodi[3] and Zhenhao Shi*[1,2]

[1]*Department of Geotechnical Engineering, Tongji University, Shanghai 200092, China*
[2]*Key Laboratory of Geotechnical and Underground Engineering of Ministry of Education, Tongji University, Shanghai 200092, China*
[3]*Department of Civil, Architectural, and Environmental Engineering, University of Texas at Austin, Austin, TX 78712, U.S.A.*

(Received April 23, 2020, Revised June 1, 2021, Accepted June 30, 2021)

Abstract. To protect adjacent buildings is a major concern for the construction of excavation in urban areas. In practice, the impacts on neighboring pile-supported buildings are normally minimized by limiting the deflection of earth retaining wall. Existing deflection criteria, however, are often empirical. In this work, we employ an analytical model to relate the wall deflection of braced excavation to the response of adjacent pile-supported buildings and thus forming a theoretical tool for determining the allowable deformation of excavation support structures based on the tolerance of buildings to distortion. The model combines closed-form excavation-induced free-field soil movements with elastic continuum solution that explicitly accounts for the interactions between raft, piles, and soils. Following validation against field model test and finite element simulation, the model is utilized to reveal the correspondence between the angular distortion of pile-supported buildings and the maximum retaining wall deflection under different combinations of excavation geometry, soil properties, and parameters of pile foundation potentially encountered in practice. A dimensionless factor composed of these influencing variables is proposed, and its correlation with the ratio of the building angular distortion over the maximum retaining wall deflection provides a rational way to determine the serviceability limit states of braced excavation.

Keywords: angular distortion; braced excavation; pile-supported building; serviceability limit state; wall deflection

1. Introduction

The motivation of this work comes from the construction of deep excavation in urban areas, where potential damage to adjacent facilities caused by excavation-induced soil movements is a major concern (Boscardin and Cording 1989, Boone *et al.* 1999, Ou *et al.* 2000, Zheng *et al.* 2017, Lee *et al.* 2018, Houhou *et al.* 2019, Hsiung 2019, Nam *et al.* 2020, Harahap and Ou 2020). In congested cities, excavations are commonly planned in the proximity of high-rise buildings that are normally supported by pile or piled raft foundations (Finno *et al.* 1991, Goh *et al.* 2003, Liyanapathirana and Nishanthan 2016, Korff *et al.* 2016, Shi *et al.* 2019, Soomro *et al.* 2019). Often in practice, ground movements caused by the excavation and the consequent damage to pile-supported buildings are controlled indirectly by limiting the deformation of earth retaining structure, noticeably the lateral deflection of earth retaining wall. The simplicity of this approach makes it appealing in practice, but its effectiveness strongly depends on the employed criteria for earth retaining wall deflection. Existing criteria, nevertheless, are often purely empirical or established by considering only the safety of the excavation. Accordingly, our objective here is to develop a rational and theoretically sound approach for determining the allowable wall deflections of braced excavation based on the tolerance of adjacent pile-supported buildings to distortion.

The intrigue and complexity of the targeted problem rest on the nonlinearity of soil stress-strain characteristics (in particular the variation of stiffness at small strain levels of 1×10^{-5} to 1×10^{-3}) (Jardin *et al.* 1986, Kim and Finno 2012, Ng *et al.* 2020, Dong *et al.* 2016), the interactions involving multi-agencies including soils and different structural components (e.g., excavation support structures, pile and raft of building foundation). All these factors result in that the modelling of this problem poses considerable challenges. Currently, the analyses of such engineering problem have largely relied on numerical techniques such as finite element method (FEM) (Finno *et al.* 1991, Burlon *et al.* 2013, Chai *et al.* 2014, Chowdhury *et al.* 2016, Soomro *et al.* 2019, Mansouri and Asghari-Kaljahi 2019, Harahap and Ou 2020). The advantages of this method rest on the capacities to consider complex soil behaviour and the evolving boundary conditions that follow construction sequences. Accurate FEM simulations normally require an extensive database to determine soil model parameters (e.g., Whittle *et al.* (1993), Dong *et al.* (2016), Pedro *et al.* (2017)) and considerable expertise on numerical methods. In many engineering projects, these prerequisites, however, are either unwarranted and infeasible. Under such conditions, theoretically sound yet simplified models which only require simple material parameters may be more appropriate choices (e.g., Hsiao *et al.* (2008), Schuster *et al.* (2009)). These analytical tools achieve a balance between

*Corresponding author, Assistant Professor
E-mail: 1018tjzhenhao@tongji.edu.cn

ISSN: 2005-307X (Print), 2092-6219 (Online)

accuracy and efficiency by focusing on the critical interactions between soil and structures and between structural components, and by incorporating soil behaviour that is representative within characteristic strain or stress ranges pertaining to the problems at hands. As a consequence, despite the inevitable simplifications, these analytical models can approximate high-fidelity simulations with an acceptable level of errors (Loganathan *et al.* 2001, Xu and Poulos 2001, Mu *et al.* 2012) and thus play an important role in both industry and academia. In this work, we will present a simple analytical model for assessing the response of piled raft foundation subjected to adjacent excavations. This model is further employed to devise a tool for determining the allowable retaining wall deflection in accordance with the tolerance of adjacent buildings to distortion

The analytical model described in the following falls in the category of displacement-controlled two-stage models (see Xu and Poulos (2001), Loganathan *et al.* (2001), Mu *et al.* (2012)). Specifically, a closed-form expression of free-field soil movements caused by excavation (i.e., the soil movements that would occur without the presence of pile foundation) is incorporated into an elastic continuum solution, through which the response of pile foundation subjected to prescribed soil displacement field is evaluated. The adopted soil displacements field accounts for the small-strain behavior of soils, while the load transfer and deformation compatibility between soil-pile, pile-pile, pile-raft, and raft-soils are explicitly considered in the continuum model. Field model test and FEM simulation are used to verify the model. Subsequently, the model is applied to study the correspondence between the angular distortion of pile-supported buildings and the deformation of earth retaining walls under different combinations of excavation geometries, soil properties and pile foundation parameters. Based on the latter analyses, a dimensionless factor composed by these variables is defined based on the roles of these variables in affecting building distortion. The correlation between this composite factor and the ratio of building angular distortion over the maximum retaining wall deflection provides a rational way to determine the serviceability limit states of braced excavation adjacent to buildings supported by pile foundation.

2. Model formulation

Fig. 1 sketches the problem studied in this work, where a rectangular excavation is constructed in the vicinity of a piled raft foundation. The ground movements caused by the excavation lead to additional deformations and internal forces of the pile foundation. The proposed analytical model utilizes a displacement-based, two-stage modelling methodology. During the first stage, free-field soil movements induced by braced excavation is calculated, which is imposed to pile foundation during the second stage to evaluate its response. To manage the complexity of the problem, the following key assumptions are made:

1. Free-field soil movements are along planes perpendicular to the retaining wall (i.e., parallel to the x-z plane in Fig. 1), and the out-of-plane soil movements (i.e., along y direction) is neglected. Consequently, only the response of pile and raft parallel to the x-z plane is considered. Such simplification is made as the soil movements perpendicular to retaining wall are usually significantly greater than that along the wall direction (Burland *et al.* 1977, Finno and Bryson 2002, Leung *et al.* 2003).

2. The piles are considered as elastic beams, while the soils as layered elastic continuum. As will become clear in the following, such proposition allows utilizing existing elasticity solutions and the principle of superposition for a linear system. These theories will be the bases of an analytical model that can quickly compute the response of piled raft due to the soil movements caused by deep excavation. Many existing studies have shown that this elasticity method can be reasonable approximation, given that the strain levels of soils are relatively small (Liang *et al.* 2017, Loganathan *et al.* 2001, Park 2004, Pinto and Whittle 2014, Leung *et al.* 2010), such as those induced by braced deep excavation focused in this work (Jardin *et al.* 1986, Whittle *et al.* 1993, Burland 1989).

3. There is no slippage and separation at the connections between piles and the raft, at the interfaces between soils and piles, and between soils and the raft. The "no slippage/separation" assumption implies that the interfaces between soils and raft/piles are rough such that the relative movements along these interfaces are negligible relative to the deformation within soils. This assumption can be considered reasonable when the raft and piles are made of reinforced concretes as commonly seen in engineering practice. This type of construction materials can develop considerably strong bonds at their interfaces with soils (Potyondy 1961, Brumund and Leonards 1973).

Note that the model formulation given as follows closely resembles those described by the authors (Mu *et al.* 2012) for analysing the problems of piles adjacent to tunnelling.

2.1 Excavation-induced free-field soil movements

The excavation-induced free-field soil movements are calculated from the closed-form expression proposed by the authors (Mu and Huang 2016):

$$u(x,y,z)=u_{\max}a_x\exp\left[-\left(\frac{3z-3H}{H+D}\right)^2-\pi\left(\frac{y}{R}\right)^2-\left(\frac{\frac{x}{z}-b_x}{c_x}\right)^2\right] \quad (1)$$

$$w(x,y,z)=\begin{cases}0.8u_{\max}a_z\left(\frac{x}{H}+0.5\right)\exp\left[-\pi\left(\frac{y}{R}\right)^2-\left(\frac{z/x-b_z}{c_z}\right)^2\right] & (0\le x\le 0.5H)\\ 0.8u_{\max}a_z\left(-0.6\frac{x}{H}+1.3\right)\exp\left[-\pi\left(\frac{y}{R}\right)^2-\left(\frac{z/x-b_z}{c_z}\right)^2\right] & (0.5H\le x\le 2H)\\ 0.8u_{\max}a_z\left(-0.05\frac{x}{H}+0.2\right)\exp\left[-\pi\left(\frac{y}{R}\right)^2-\left(\frac{z/x-b_z}{c_z}\right)^2\right] & (2H\le x\le 4H)\end{cases} \quad (2)$$

where $u(x,y,z)$ and $w(x,y,z)$ denote horizontal and vertical soil displacements along the planes perpendicular to the retaining wall, respectively (note that the employed

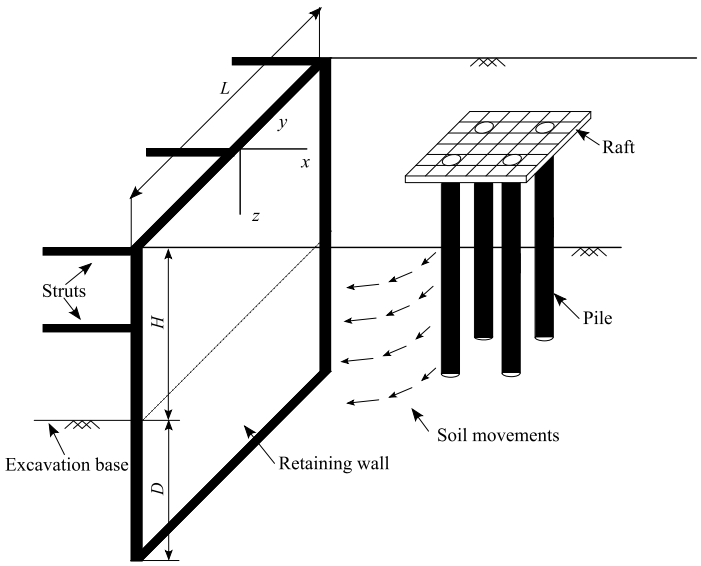

Fig. 1 Schematics illustrating the problem of piled raft deforming due to soil movements caused by adjacent deep excavation.

Cartesian coordinate x, y, and z is shown in Fig. 1 and the origin is at the top of the center line of the retaining wall). In these equations, u_{max} is the maximum lateral deflection of the earth retaining wall, i.e. the focused indicator for the deformation of earth retaining system. $R = L[0.069 \ln(H/L) + 1.03]/2$ is the equivalent excavation length, and H, L, D the excavation depth, the retaining wall length, and the embedded depth (see Fig. 1). The coefficients a_x, b_x, c_x, a_z, b_z, and c_z are functions of the spatial coordinates of soils and the sizes of the excavation:

$$\begin{aligned} a_x &= 1+\exp(-10.47\frac{z}{H}+0.76) \\ b_x &= \exp(-6.45\frac{z}{H}+2.76) \\ c_x &= \exp(-2.86\frac{z}{H}+2.64) \\ a_z &= 1+\exp(-1.56\frac{x}{H}-1.68) \\ b_z &= \exp(-2.56\frac{x}{H}+1.02) \\ c_z &= \exp(-2.09\frac{x}{H}+1.75) \end{aligned} \tag{3}$$

The construction of Eqs. (1) and (2) involves fitting the results of finite element simulations based on the well-established Hardening Soil Small model (Benz 2007). This model explicitly considers the non-linear variation of soil stiffness at small strains that has proven to be critical in accurately assessing the ground movements associated with deep excavations (Jardin *et al.* 1986, Atkinson 2000). The usefulness of these equations is highlighted by the fact that the free-field soil displacements can be estimated immediately once the maximum retaining wall deflection is known.

2.2 Response of piled-raft

In the second stage of the analysis, the response of piled-raft subjected to the displacement field of Eqs. (1) and (2) is computed. For this purpose, an elastic continuum solution including soils, pile, raft as interaction agencies is developed. In the model, the general force equilibrium of the raft can be represented by

$$\mathbf{R} = \sum_{i=1}^{m} \mathbf{J_i P_i} + \sum_{j=1}^{n} \mathbf{I_i S_i} \tag{4}$$

where the vector $\mathbf{R} = \{T, M, Q\}^T$ contains the external shear force T, moment M and axial force Q acting on the raft that are transferred from the building, while the first and second parts of the RHS of Eq. (4) denote the forces transferred from the connected piles and underlying soils, respectively. In particular, the vector $\mathbf{P_i} = \{T_i, M_i, Q_i\}^T$ denotes the internal forces transferred from the i^{th} pile of the total m piles, while the vector $\mathbf{S_i} = \{T_j^s, Q_j^s\}^T$ contains the shear and normal forces transferred from the j^{th} soil element out of the totally n soil elements that interact with the raft, as illustrated in Fig. 2(a). The matrixes $\mathbf{J_i}$ and $\mathbf{I_i}$ are functions of coordinates of the piles and soil elements:

$$\mathbf{J_i} = \begin{bmatrix} 1 & 0 & 0 \\ 0 & 0 & x_i - x_1 \\ 0 & 0 & 1 \end{bmatrix} \tag{5}$$

and

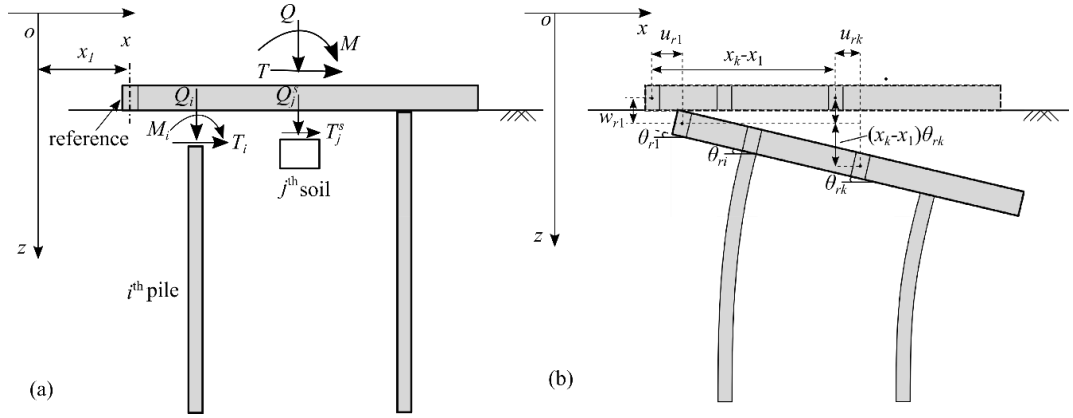

Fig. 2 Schematics illustrating the statics and kinematics of piled raft: (a) force equilibrium of the raft subjected to external actions and internal forces transferred between raft and piles, and between raft and underlying soils and (b) rigid-body motions of the raft and the corresponding displacements compatibility between different raft elements

$$\mathbf{I_i} = \begin{bmatrix} 1 & 0 \\ 0 & x_j - x_1 \\ 0 & 1 \end{bmatrix} \tag{6}$$

In Eqs. (5) and (6), x_i and x_j denote the x coordinate of the i^{th} pile and j^{th} soil element, respectively, while x_1 is the x coordinate of a reference raft element (see Fig. 2) to compute the moments generated by axial (normal) forces (i.e., Q_i and Q^s_j).

By assuming that no separation is allowed between raft, pile heads and the attached soils, we obtain the following compatibility conditions:

$$\begin{aligned} u_{rk} &= u_{sk} + u_{fk} \\ \theta_{rk} &= \theta_{sk} + \theta_{fk} \\ w_{rk} &= w_{sk} + w_{fk} \end{aligned} \tag{7}$$

As shown in Fig. 2(b), u_{rk}, θ_{rk} and w_{rk} denote the horizontal movement, rotation and vertical settlement of the k^{th} raft element, while the subscript sk and fk indicate the motions of pile heads (or soil elements) attached to the k^{th} raft element, due to the soil movements of Eqs. (1) and (2) and force transfer, respectively. Here the total number of raft elements equals to $m + n$, i.e., the summation of the number of piles m and the number of underlying soil elements n. Fig. 1 illustrates how the number of these elements is determined. Specifically, the raft is discretized by a mesh with square elements, whose size coincides with the diameter of piles. The soil domain underlying the raft is discretized by the elements of the same size. Accordingly, the number of soil elements is equal to the total number of raft elements minus the number of piles (i.e., those raft elements that are connected to piles rather than in contact with soils). This method to discretize the raft and soils has the advantage that it can be relatively straightforwardly extended to piled raft with different plan-view configurations and number of piles.

We further assume that the raft only exhibits rigid-body motions. Accordingly, the motions of raft elements u_{rk}, θ_{rk} and w_{rk} in Eq. (7) can be fully specified by knowing the rotation of the raft as well as the horizontal and vertical displacements of a reference element along on the raft, as shown in Fig. 2(b). The latter can be expressed as

$$\begin{aligned} u_{rk} &= u_{r1} \\ \theta_{rk} &= \theta_{r1} \\ w_{rk} &= w_{r1} + (x_k - x_1)\theta_{rk} \end{aligned} \tag{8}$$

where θ_{r1} is degree of rotation of the raft, u_{r1} and w_{r1} denote the horizontal and vertical movements of the reference raft element, while x_1 and x_k are the x coordinate of the reference and the k^{th} raft element, respectively. It should be noted that the rigid body assumption can be considered reasonable for typical rafts in engineering practice, which are often composed of reinforced concrete structures with relatively large heights (Reul and Randolph 2003, Sinha and Hanna 2017, Poulos 2001, Prakoso and Kulhawy 2001). The high stiffness of the raft relative to that of the soils and piles can result in that the deformation of the raft is much small compared with that within piles and soils. On the other hand, it should be noted that this rigid body assumption might not be appropriate for piled rafts with considerably large plan-view dimensions, where the compliance of the raft might need to be considered in the analysis.

By substituting Eq. (8) into (7), we obtain $3m + 3n$ equations. By assuming that the rotation rigidity of soil elements attached to the raft is negligible (i.e., the equation $\theta_{rk} = \theta_{sk} + \theta_{fk}$ is only evaluated for pile heads), we further reduce the number of equations to $3m+2n$. The latter, assembled with the raft force equilibrium of Eq. (4), leads to a system of $3m + 2n + 3$ equations with the same numbers of unknowns (i.e., the internal forces T_i, M_i and Q_i for m piles, the internal forces T^s_j and Q^s_j for n attached soil elements, the external forces T, M, and Q, or equivalently the movements of the reference raft element θ_r, u_{r1} and w_{r1}). Such linear system can be expressed as the following compact matrix form:

$$\begin{Bmatrix} \mathbf{R} \\ \mathbf{J^T U - G} \\ \mathbf{I^T U - K} \end{Bmatrix} = \begin{bmatrix} \mathbf{J} & \mathbf{I} & \mathbf{0} \\ \mathbf{A} & \mathbf{C} & \mathbf{0} \\ \mathbf{D} & \mathbf{B} & \mathbf{0} \end{bmatrix} \begin{Bmatrix} \mathbf{P} \\ \mathbf{S} \\ \mathbf{U} \end{Bmatrix} \tag{9}$$

where the sub-vector $\mathbf{P}=\{\mathbf{P_1},...,\mathbf{P_i},...,\mathbf{P_m}\}^T$ contains the internal forces at pile heads (i.e., $\mathbf{P_i},=\{T_i,M_i,Q_i\}^T$), $\mathbf{S}=\{\mathbf{S_1},...,\mathbf{S_j},...,\mathbf{S_n}\}^T$ includes the transferred forces between the raft and underlying soil elements (i.e., $\mathbf{S_i}=\{T_j^s,Q_j^s\}^T$), $\mathbf{R}=\{T,M,Q\}^T$ denotes the external forces and moments acting on the raft that are transferred from the superstructure. Accordingly, the first row of Eq. (9) describes the force equilibrium of the raft. The product $\mathbf{J^TU}$ in the second row evaluates the movements of the raft elements that are attached to pile heads (i.e., also the pile head movements) by employing the rigid-body motion of Eq. (8). The displacements and rotation of the reference raft element are given in $\mathbf{U}=\{u_{r1},\theta_{r1},w_{r1}\}^T$, while $\mathbf{J}=[\mathbf{J_1},...,\mathbf{J_i},...,\mathbf{J_m}]$ denotes the transformation matrix with $\mathbf{J_i}$ defined in Eq. (5). The sub-vector $\mathbf{G}$ contains the movements of pile heads solely due to excavation-induced displacement field, in that $\mathbf{G}=\{\mathbf{G_1},...,\mathbf{G_i},...,\mathbf{G_m}\}^T$ with $\mathbf{G_i}=\{u_{si},\theta_{si},w_{si}\}^T$. Accordingly, the vector $\mathbf{J^TU}-\mathbf{G}$ gives the movements of pile heads due to the internal axial force, shear force and moment transferred between the raft, piles and surface soil elements, i.e., those included in **P** and **S**. The matrices **A** and **B** in Eq. (9) are the flexibility matrices that related pile head motions to the internal forces mentioned above, and their expressions will be discussed in the following. Similarly, the operation $\mathbf{I^TU}$ evaluates the vertical and horizontal displacements of the raft elements that are supported by soils (also the displacements of these soil elements), and the components of the transformation matrix $\mathbf{I}=[\mathbf{I_1},...,\mathbf{I_j},...,\mathbf{I_n}]$ is given in Eq. (6). The sub-vector $\mathbf{K}=\{\mathbf{K_1},...,\mathbf{K_j},...,\mathbf{K_n}\}^T$ with $\mathbf{K_j}=\{u_{sj},w_{sj}\}^T$ denotes the movements of these underlying soil elements induced by excavation, while $\mathbf{I^TU}-\mathbf{K}$ gives the displacements of these soil elements due to internal forces contained in **P** and **S**. **C** and **D** denote the corresponding flexibility matrices.

Mu *et al.* (2012) analyse the response of pile group in layered elastic continuum induced by prescribed soil movements and show that the element of the vector **G** can be expressed as

$$\mathbf{G_i}=\begin{Bmatrix}u_{si}\\ \theta_{si}\\ w_{si}\end{Bmatrix}=\begin{Bmatrix}u_{si}^0\left(1-\sum_{k=1,k\neq i}^{m}\rho_{us}^{ik}\right)\\ \theta_{si}^0\left(1-\sum_{k=1,k\neq i}^{m}\rho_{\theta s}^{ik}\right)\\ w_{si}^0\left(1-\sum_{k=1,k\neq i}^{m}\rho_{ws}^{ik}\right)\end{Bmatrix} \tag{10}$$

where u_{si}^0, θ_{si}^0, and w_{si}^0 denote the motions at the head of the i^{th} pile caused by excavation-induced soil displacements when interactions between piles are ignored. ρ_{us}^{ik}, $\rho_{\theta s}^{ik}$, and ρ_{ws}^{ik} are pile-pile interaction factors that account for the reduction on pile movements due to the presence of other piles. To obtain the values of u_{si}^0, θ_{si}^0, and w_{si}^0, we solve the response of a standalone pile by finite difference method combined with the displacement and stress solutions for asymmetric loads in layered elastic continuum. The pile-pile interaction factors are evaluated by using the same approach but with respect to a pair of piles. Detailed solution procedures are well documented in Poulos and Davis (1980), Mu *et al.* (2012).

Similarly, the element of the vector $\{\mathbf{K}\}$ is given by

$$\mathbf{K_j}=\begin{Bmatrix}u_{sj}\\ w_{sj}\end{Bmatrix}=\begin{Bmatrix}u_{sj}^0\left(1-\sum_{k=1}^{m}\gamma_{us}^{jk}\right)\\ w_{sj}^0\left(1-\sum_{k=1}^{m}\gamma_{ws}^{jk}\right)\end{Bmatrix} \tag{11}$$

Here the quantities u_{sj}^0 and w_{sj}^0 denote vertical and horizontal displacements of the j^{th} soil elements beneath the raft caused by excavation. Again, the superscript 0 indicates that such soil movements ignore the presence of piles, thus can be directly evaluated from Eqs. (1) and (2). γ_{us}^{jk} and γ_{ws}^{jk} are pile-soil interaction factors that account for the reduced soil displacements due to the presence of piles. We obtain these factors by solving the system consisting of a single pile and layered elastic medium (Mu *et al.* 2012).

The matrix **A** itself can be partitioned into $m \times m$ blocks (here m is the number of piles). Each block $\mathbf{A}_{pq}$ defines the motions of the p^{th} pile head, including horizontal and vertical displacements and rotations, due to unit axial force, moment, and shear force acting on the q^{th} pile heads:

$$\mathbf{A}_{pq}=\begin{cases}\begin{bmatrix}\alpha_{uT}^{pq}u_T^0 & \alpha_{uM}^{pq}u_M^0 & 0\\ \alpha_{\theta T}^{pq}\theta_T^0 & \alpha_{\theta M}^{pq}\theta_M^0 & 0\\ 0 & 0 & \alpha_{wQ}^{pq}w_Q^0\end{bmatrix} & p\neq q\\ \begin{bmatrix}\alpha_{uT}^{pq}u_T^0 & \alpha_{uM}^{pq}u_M^0 & 0\\ \alpha_{\theta T}^{pq}\theta_T^0 & \alpha_{\theta M}^{pq}\theta_M^0 & 0\\ 0 & 0 & \alpha_{wQ}^{pq}w_Q^0\end{bmatrix}-\sum_{k=1,k\neq p}^{m}\begin{bmatrix}\omega_{uT}^{pk}u_T^0 & \omega_{uM}^{pk}u_M^0 & 0\\ \omega_{\theta T}^{pk}\theta_T^0 & \omega_{\theta M}^{pk}\theta_M^0 & 0\\ 0 & 0 & \omega_{wQ}^{pk}w_Q^0\end{bmatrix} & p=q\end{cases} \tag{12}$$

where u_T^0 and u_M^0 denote the horizontal displacement of the head of a standalone pile subjected to unit shear force and unit moment acting the head, respectively; θ_T^0 and θ_M^0 indicate the rotation of the head of the standalone pile subjected to the unit shear force and unit moment, respectively; and w_Q^0 denotes the vertical settlement of the standalone pile due to unit axial force acting on the pile head. These pile head movements can be solved from the linear system composed of a single elastic pile beam embedded in layered elastic continuum, and form the base solutions. The factors α^{pq} and ω^{pk} are scaling factors operating on these base solutions to account for the pile-pile interactions. In particular, α^{pq} denotes the scaling factor to

attain the pile head movements associated with the p^{th} pile induced by the internal forces acting on the the q^{th} pile. Accordingly, α^{pq}=1 when p=q. The factors ω^{pk} describe the shielding effects, i.e., the reduction of active soil movements (e.g., those induced by deep excavation of Eqs. (1) and (2)) due to the presence of piles (Lam *et al.* 2013, Huang *et al.* 2009). In particular, the superscript pk indicates the attenuation of soil displacements at the location of the p^{th} pile due to the presence of the k^{th} pile. Note that Eq. (12) implies that such reduction on soil movements is included only in the diagonal components of the flexibility matrix of Eq. (12) (i.e., p=q), which relates the displacements and internal forces of the same pile. This is because these shielding effects are only needed to be accounted for for one time for each pile. The factors α^{pq} and ω^{pk} can be evaluated by analysing a pair of piles embedded in elastic medium following the procedures documented in Mu *et al.* (2012).

The matrix **B** is used to compute the displacements of the soil elements beneath the raft due to the forces transferred between the raft and the soils. Similar to the matrix **A**, we can partition **B** into $n \times n$ blocks, with n the total number of soil elements. Each of these blocks, $\mathbf{B}^{pq}$, quantifies the movements of the p^{th} soil elements due to unit normal and shear forces acting on the q^{th} soil element:

$$\mathbf{B}_{pq} = \begin{cases} \begin{bmatrix} \xi_{uT}^{pq} u_{sT}^{0} & 0 \\ 0 & \xi_{wQ}^{pq} w_{sQ}^{0} \end{bmatrix} & p \neq q \\ \begin{bmatrix} \xi_{uT}^{pq} u_{sT}^{0} & 0 \\ 0 & \xi_{wQ}^{pq} w_{sQ}^{0} \end{bmatrix} - \sum_{k=1}^{m} \begin{bmatrix} \zeta_{uT}^{pk} u_{sT}^{0} & 0 \\ 0 & \zeta_{wQ}^{pk} w_{sQ} \end{bmatrix} & p = q \end{cases} \tag{13}$$

where the base solutions u_{sT}^{0} denotes the horizontal displacements of a soil surface element when subjected to a unit shear force, while w_{sQ}^{0} represents the vertical displacements of a soil element when a unit axial force is acting on it. These base solutions are used, in combination with the scaling factors ξ^{pq}, to obtain the displacements of the p^{th} soil element in response to the forces acting on the q^{th} soil element. The factors ζ^{pk} account for the shielding effects on the p^{th} soil element due to the presence of the k^{th} pile. Similar to the inclusion of sheilding effects for pile displacements (see Eq. (12)), these effects are only needed to be accounted for once for each soil element (i.e., when p=q). The base solutions u_{sT}^{0} and w_{sQ}^{0} can be obtained by solving the response of an elastic medium subjected to pointed loads, while the scaling factors ξ^{pq} and ζ^{pk} can be evaluated by analysing the linear system composed by a single pile embedded in an elastic medium. For detailed solution procedures, we refer the readers to existing literatures such as Mu *et al.* (2012).

The matrices **C** and **D** describe the coupling between piles and surface soil elements. **C** can be partitioned into $m \times n$ blocks, with each block $\mathbf{C}_{pq}$ defining the motions of the p^{th} pile head due to the normal and shear force acting on the q^{th} soil element:

Table 1 Model input parameters and their values for the baseline case in parametric study

Parameters	Unit	Value
Excavation depth, H	m	10
Embedment depth, D	m	10
Excavation length, L	m	40
Young's Modulus of soils, E_s	MPa	24
Poisson's ratio of soil, v_s	/	0.3
Young's Modulus of pile, E_p	GPa	30
Poisson's ratio of pile, v_p	/	0.167
Pile length, l	m	25
Pile diameter, d	m	0.8
Raft-excavation spacing, s	m	3.2
Pile spacing, s_0	m	2.4

$$\mathbf{C}_{pq} = \begin{bmatrix} \beta_{uT}^{pq} u_{T}^{0} & 0 \\ \beta_{\theta T}^{pq} \theta_{T}^{0} & 0 \\ 0 & \beta_{wQ}^{pq} w_{Q}^{0} \end{bmatrix} \tag{14}$$

The matrix **D** can be partitioned into $n \times m$ blocks. Each of these blocks, $\mathbf{D}_{pq}$, quantities the displacements of the p^{th} soil elements due to internal forces acting on the q^{th} pile head:

$$\mathbf{D}_{pq} = \begin{bmatrix} \kappa_{uT}^{pq} u_{sT}^{0} & \kappa_{uM}^{pq} u_{sT}^{0} & 0 \\ 0 & 0 & \kappa_{wQ}^{pq} w_{sQ} \end{bmatrix} \tag{15}$$

The scaling factors β^{pq} and κ^{pq} can be obtained by solving the interaction between a single pile and soil elements lying on the top surface of an elastic continuum in accordance with the procedures described in Mu *et al.* (2012).

2.3 Model input parameters

Table 1 summarizes the input parameters for the analytical model described above. Note that the pile spacing is center-to-center distance, while the raft-excavation spacing is the distance between the edge of the excavation to the center of the raft along the direction perpendicular to the retaining wall.

3. Model verification

The two-stage model described above is implemented in a Fortran code, hereafter will be referred to as APPR. The verification of the model is performed with respect to the examples of single pile and piled raft adjacent to excavation as follows.

3.1 Response of single pile adjacent to excavation

Goh *et al.* (2003) report the results of a full-scale, three-

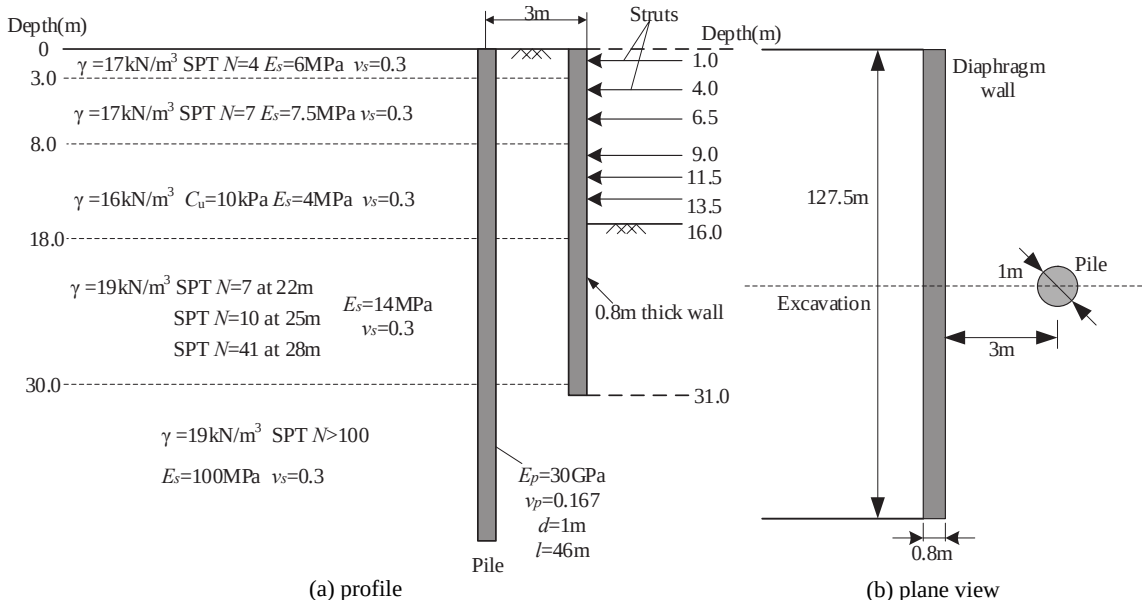

Fig. 3 Soil profile and test configuration in the field test of the response of single pile adjacent to a braced excavation (Goh *et al.* 2003). Note that the Young's modulus of soils E_s are converted from the reported SPT N values or unconfined compressive strength C_u, while the Poisson's ratio v_s = 0.3 is assumed for all soil strata

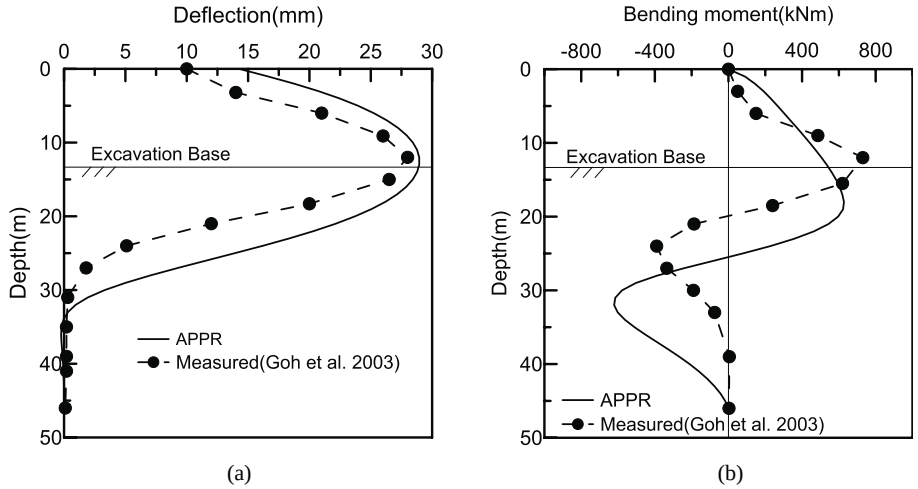

Fig. 4 Comparison between measured and computed pile response: (a) lateral deflection and (b) bending moment

dimensional field model test on the response of a single pile induced by a nearby excavation, as sketched in Fig. 3. The excavation is 16 m deep, made into five soil strata, and is supported by a 0.8 m thick diaphragm wall and six struts. The 1 m diameter pile is 46 m long and 3 m away from the retaining wall. Fig. 3 provides the basic mechanical properties of soil layers involved, as well as the derived soil parameters in accordance with the correlations suggested by Goh *et al.* (1997). Fig. 4 compares the measured and computed pile lateral deflection and bending moment that correspond to a maximum wall deflection u_{max} of 29 mm. A reasonably good agreement is seen, even if the computed location with zero bending moment is lower than that observed.

3.2 Response of piled raft adjacent to excavation

Field measurements or model tests concerning the response of piled raft caused by adjacent braced excavation are scarce in the literature. Thus, a three-dimensional finite element simulation is performed to assess the proposed model. As shown in Fig. 5, the excavation is 15 m deep and made through strata consisting of six layers of clay. The support system is composed of a 0.91 m thick and 21 m long slurry wall and five concrete struts. A square-shaped raft is connected to four 0.8 m diameter and 25 m length pile, and the space between pile center is 2.4m. The center of the raft is 4.2 m away from the excavation. Simulations are carried out in Plaxis 3D using the hardening soil model with small-strain stiffness. A detailed discussion of soil parameters and FEM modelling procedures can be found in Mu and Huang (2016). The response of the piled raft computed using the proposed model and FEM are compared in Fig. 6, which corresponds to a maximum retaining wall deflection u_{max} of 30 mm. The soil and pile parameters used in the analytical model are provided in Fig. 5. It is seen that

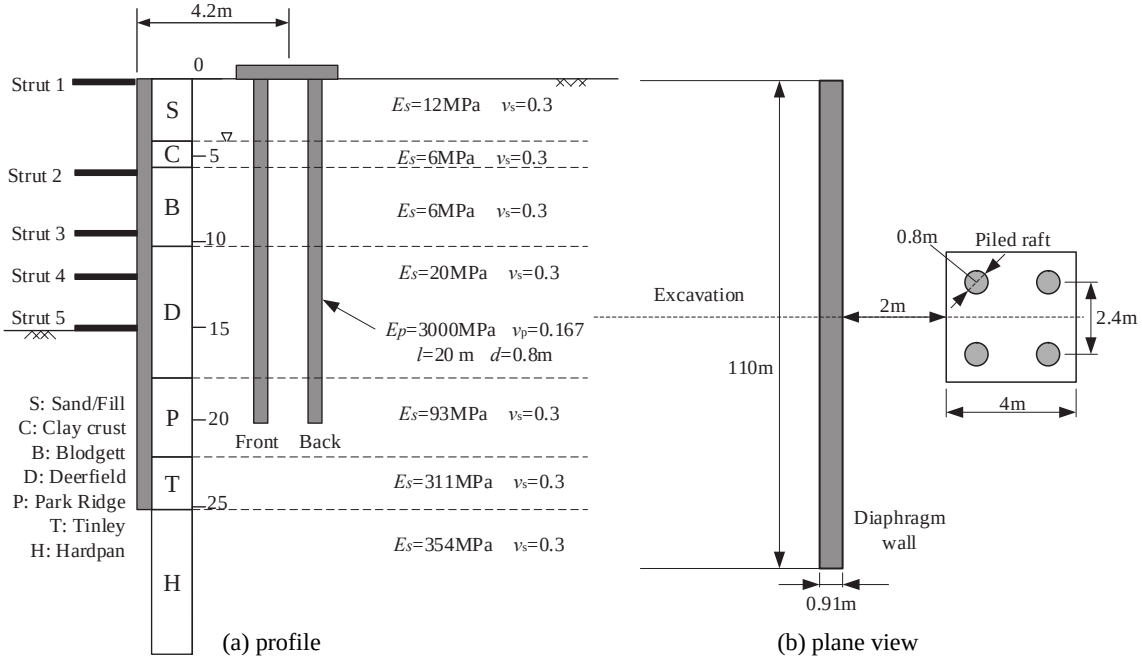

Fig. 5 Soil profile and test configuration in the synthetic case study of the response of piled-raft adjacent to a braced excavation

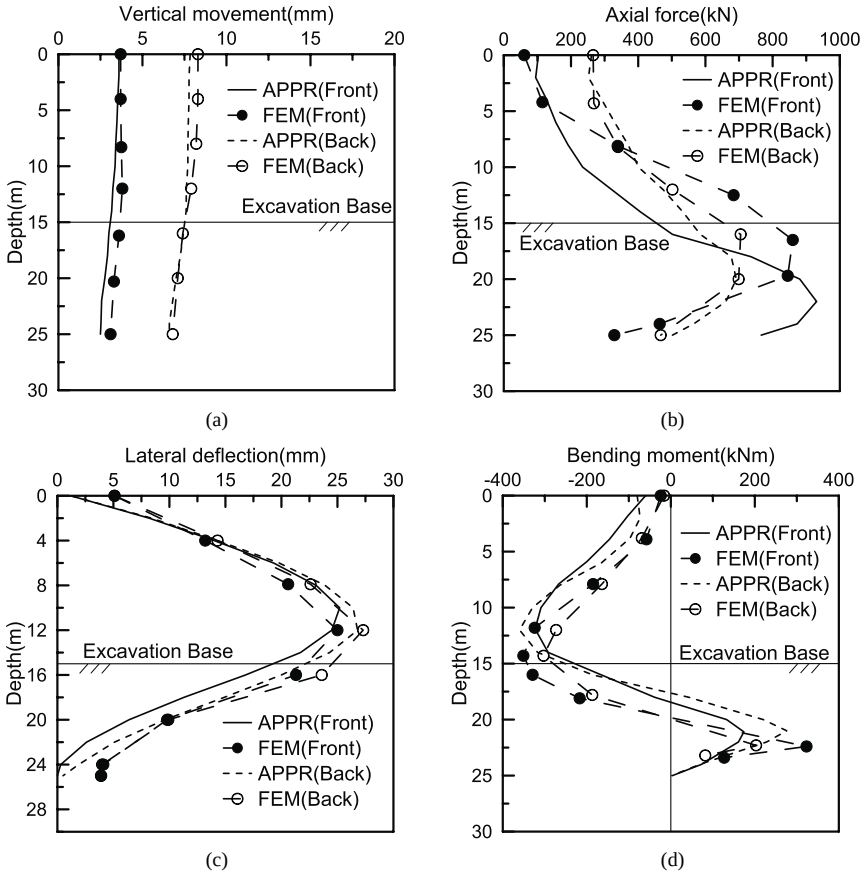

Fig. 6 Comparison between computed pile response by FEM and the proposed analytical model (APPR): (a) vertical movement, (b) axial force, (c) lateral deflection and (d) bending moment

the results obtained by using the simplified model reasonably match that computed by FEM. As an important indicator of foundation movements, the rotation of the raft computed as the ratio of the differential settlement between the front and back piles over their distance is 1.8‰ (FEM) and 1.7‰ (the analytical model). Nevertheless, quantitative

mismatches can also be observed, like the depths of peak axial force and peak bending moments are respectively overestimated and underestimated by the simple model.

4. Determination of allowable retaining wall deflection

The analytical model described above is capable of relating the deformations of excavation support structures to the response of adjacent pile foundation. In this section, we will show how such a model can be utilized to construct a simple approach enabling practicing engineers to estimate the allowable deformations of earth retaining structures based on the tolerance of adjacent pile-supported buildings to distortion. Following engineering practice, we select the maximum wall deflection $u_{\max}$ as the deformation indicator of earth retaining structures, while the one for buildings is the angular distortion at the foundation level δ, as its magnitude is closed related to building damage (Skempton and MacDonald 1956, Wroth and Burland 1974, Boscardin and Cording 1989, Finno and Bryson 2002, Dalgic *et al.* 2018). In the following, a closed-form correlation between δ and $u_{\max}$ will be formed such that one can assess the allowable retaining wall deflections by knowing the tolerance to distortion of the buildings under protection. Because the correspondence between the deformations of earth retaining system and nearby buildings depends on various factors, like excavation geometries, soil properties, and pile parameters, we construct the correlation mentioned above by performing a parametric analysis. The influencing variables considered include excavation depth H and length L, Young's modulus of soil E_s and pile E_p, pile length l, diameter d, spacing s_0 and the distance from the excavation s. Table 1 summarizes the values of these parameters that correspond to the baseline case. In the analyses, we assume that the embedded depth of the retaining wall is equal to the excavation depth, as commonly adopted in practice, and the Poisson's ratio of soil and pile is constant. The maximum deflection of the retaining wall $u_{\max}$ ranges from 0.5%H to 4%H.

Typical building foundations normally can consist of a large number of piles and feature highly variable plan-view shapes. Therefore, a generic piled foundation is required before we can draw any general correlation between δ and $u_{\max}$ that is applicable to different engineering projects. In this analysis, a building foundation composed of a square-shaped raft and four piles is considered (see Fig. 1). This pile group is the minimal element enabling the evaluation of the building angular distortion along two mutually orthogonal directions. Accordingly, the angular distortion discussed in the following can be interpreted as an indicator of local building deformation, which can be critical for structures with a large footprint. Three pile head constraints are considered here, including free-head pile group (i.e., no raft), capped-head pile group (i.e., the raft is not touching the ground surface), and piled raft (i.e., the raft contacts the ground surface). In particular, the free-head pile group and capped-head pile group can be modelled by assigning the matrices $\mathbf{P}=\mathbf{0}$, $\mathbf{S}=\mathbf{0}$ and $\mathbf{S}=\mathbf{0}$, respectively, to Eq. (9).

Fig. 7 presents the typical results generated by the parametric analyses, where there exists an approximately linear relation between the building angular distortion δ and the maximum retaining wall deflection $u_{\max}$. This trend is seen from other sets of results, which allows us to focus on the influences of different variables on the ratio $\delta/u_{\max}$, as depicted in Fig. 8 (note that the dimensionless group $(\delta H)/u_{\max}$ is used in organizing the data and hereafter will be referred to as normalized angular distortion). Fig. 8 shows that, in general, the normalized angular distortion decreases with the increase in the pile modulus, pile diameter, pile length, and the spacing between piles, and with the decrease in the distance between the building foundation and the excavation. In the contrast, the angular distortion becomes larger when soil is stiffer (this finding seems to be counterintuitive at first sight and can be attributed to the fact that the piles have to comply with prescribed soil movements and stiffer soil will imply greater soil reactions acting on the piles), or when the excavation depth or length is greater. Due to complex soil-structure interactions, there are exceptions to the general rules described above. For example, the angular distortion that corresponds to the free-head pile group increases when the piles become stiffer (see Fig. 8(a)) or when soil becomes softer (see Fig. 8(b)). A possible explanation is that the piles in free-head pile group can deform more independently to each other than that in a pile group with a raft, and thus the increase in the stiffness of piles relative to the surrounding soil will enhance the differential settlements between individual piles induced by non-uniform ground movements caused by excavation.

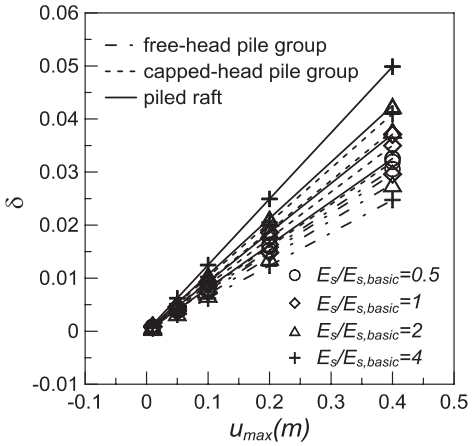

Fig. 7 Example of results computed from the parametric analysis (here the influence of Young's modulus of soil is presented). Note that $E_{s,\text{basic}}$ denotes the Young's modulus of soils that corresponds to the baseline case given in Table 1

Based on the general trends described above, we propose a dimensionless composite factor

$$I_f = \frac{E_p d l_0 s_0 s^2}{E_s L H^4} \tag{16}$$

and correlate it with the normalized angular distortion computed in the parametric study, as shown in Fig. 9. The scattered data clouds of 165 cases fall within a band, whose

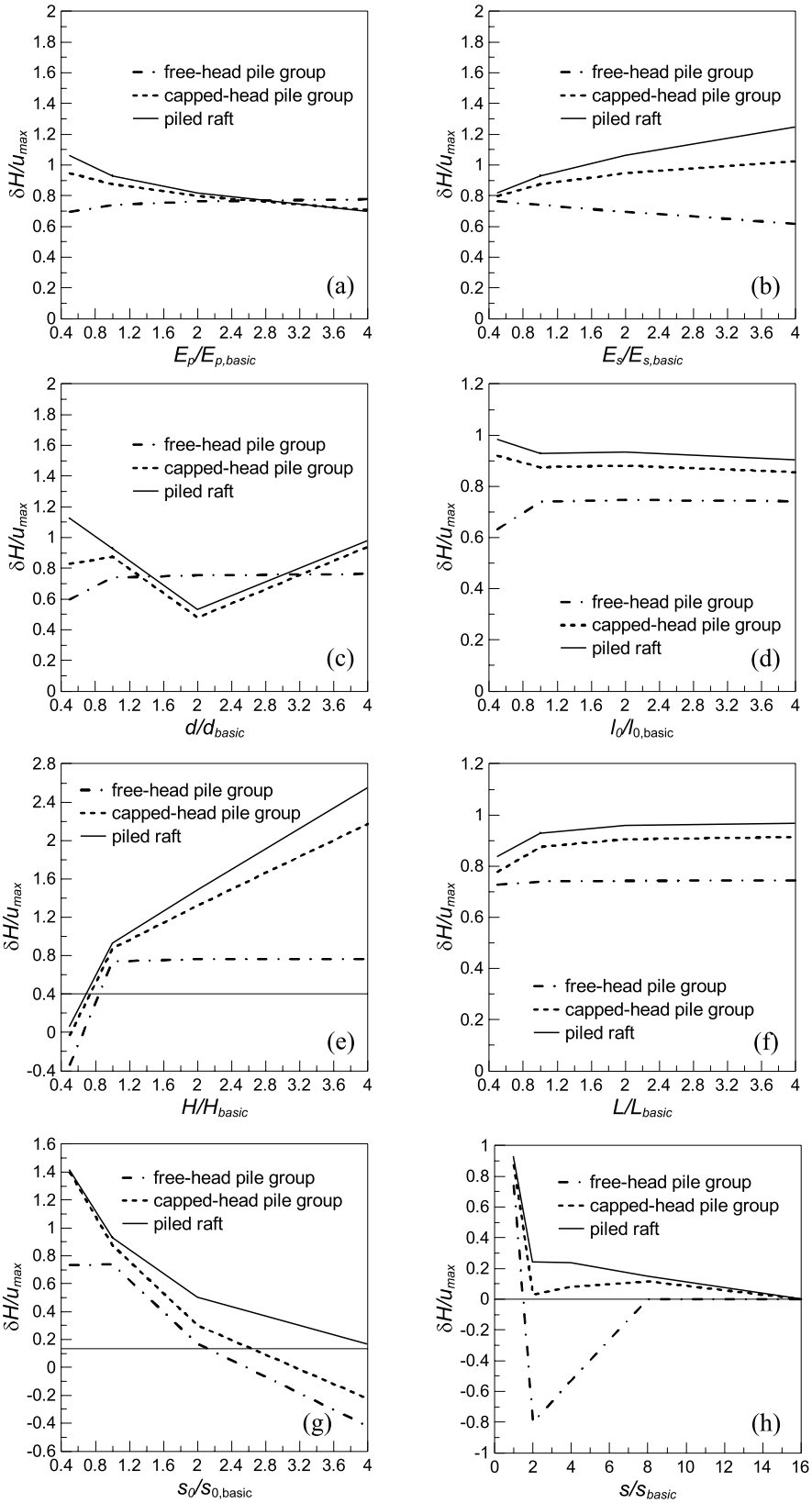

Fig. 8 Normalized angular distortion under varying: (a) pile modulus, (b) soil modulus, (c) pile diameter, (d) pile length, (e) excavation depth, (f) excavation length, (g) pile spacing and (h) distance between excavation and pile foundation

bandwidth is considered acceptable for engineering practice, given the number of influencing factors involved.

The boundaries of the band are given by

$$\left|\frac{\delta H}{u_{\max}}\right| = -\frac{3}{5}\log\left(I_f\right) + \frac{2}{5} \tag{17}$$

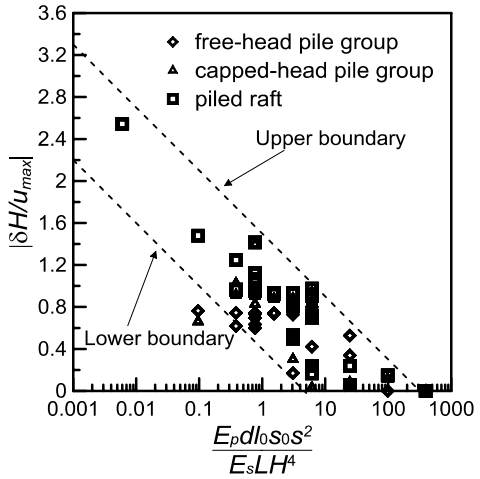

Fig. 9 Correlation between composite factor I_f and normalized angular distortion

Table 2 Allowable angular distortion for different combinations of building and foundation types (BH*: Building height)

Type of building/foundation	DGJ08-11-2010 (2010)	Finno and Bryson (2002)	Skempton and MacDonald (1956)
Masonry structures /strip foundation	0.004	NA	1/300
Frame structures /independent foundation	0.003	1/1000	1/300
Frame structures /raft foundation	0.004	1/1000	1/300
Frame structures /pile foundation	0.003～0.004	1/1000	NA
High-rise building (BH*<100m) /pile foundation	0.002～0.004	NA	NA
High-rise building (BH>100m) /pile foundation	0.001～0.002	NA	NA
Tower building (BH<100m) /pile foundation	0.005～0.008	NA	NA
Tower building (BH>100m) /pile foundation	0.002～0.004	NA	NA

and

$$\left|\frac{\delta H}{u_{\max}}\right| = -\frac{3}{5}\log\left(I_f\right) + \frac{3}{2} \tag{18}$$

Accordingly, the range of allowable retaining wall deflection that corresponds to given angular distortions of pile-supported buildings can be estimated through

$$u_{\text{allowable}} = \left(\frac{H}{-\frac{3}{5}\log\left(I_f\right) + \frac{3}{2}} \sim \frac{H}{-\frac{3}{5}\log\left(I_f\right) + \frac{2}{5}} \right) \delta_{\text{allowable}} \tag{19}$$

where $\delta_{\text{allowable}}$ and $u_{\text{allowable}}$ denote the allowable angular distortion of the buildings under protection and corresponding allowable retaining wall deflection. The former information can be found in the literature or design codes. Examples of angular distortion criteria for various types of buildings and foundations are given in Table 2.

5. Conclusions

This paper presents a method to determine the allowable retaining wall deflection of braced excavation from the perspective of protecting adjacent pile-supported buildings. A simple analytical model is given to relate the maximum retaining wall deflection to the foundation movements of adjacent buildings. This is achieved by combining a closed-form expression of excavation-induced free-field soil movements with an elastic continuum solution where the response of pile foundation subjected to prescribed soil displacement field is computed. The analytical model is verified against field model test and FEM simulation. A parametric analysis is performed by using the model, where the relation between the maximum retaining wall deflection and the angular distortion of pile-supported buildings under varying excavation geometries, soil properties, and pile parameters is studied. A dimensionless factor composed of these variables is defined based on their roles revealed from the parametric analysis, and a correlation between the composite factor and the building angular distortion normalized by the maximum wall deflection is formed. The latter provides a rational way to determine the allowable deformation of earth retaining structures in accordance with the tolerance of adjacent pile-supported buildings to distortion.

It should be emphasized that the current work represents a first step towards the development of simple yet theoretically sound approaches for determining the serviceability limit states for the construction of braced excavation in urban areas. In view of the complexity of the focused soil-structure interaction problem, there are aspects of the proposed model that should be improved in the future. For example, currently, the raft foundation is assumed to be rigid in the analytical model and its displacements coincide with the underlying soils and attached piles. Because the stiffness of raft in relative to the underlying soil may significantly impact the deformation pattern of buildings, the influences on the proposed correlation induced by the rigidity of raft should be investigated in the future. Further steps should be undertaken also to reduce the scattering in the correlation concerning building angular distortion, possibly by refining the composite factor (e.g., to incorporate the types of pile-raft connection). Lastly, unlike the proposed analytical model, we do not yet have field measurements enabling the validation of the correlation between the building angular distortion and the composite factor. The collection of field data for assessing and/or improving the correlation, therefore, will be a topic for future research.

Acknowledgments

This material is based upon work supported by the National Natural Science Foundation of China under Grant No. 51738010, the National Key R&D Program of China under Grant No. 2016YFC0800200, the Shanghai Science and Technology Committee Rising-Star Program under Grant No. 19QC1400500, and Fundamental Research Funds for the Central Universities.

References

Atkinson, J.H. (2000), "Non-linear soil stiffness in routine design", *Géotechnique*, **50**(5), 487-508. https://doi.org/10.1680/geot.2000.50.5.487.

Benz, T. (2007), "Small-strain stiffness of soils and its numerical consequences", Ph.D. Dissertation, University Stuttgart, Stuttgart, Germany.

Boone, S. J., Westland, J. and Nusink, R. (1999), "Comparative evaluation of building responses to an adjacent braced excavation", *Can. Geotech. J.*, **36**(2), 210-223. https://doi.org/10.1139/t98-100.

Boscardin, M.D. and Cording, E.J. (1989), "Building response to excavation-induced settlement", *J. Geoteh. Eng.*, **115**(1), 1-21. https://doi.org/10.1061/(ASCE)0733-9410(1989)115:1(1).

Burlon, S., Mroueh, H. and Shahrour, I. (2013), "Influence of diaphragm wall installation on the numerical analysis of deep excavation", *Int. J. Numer. Anal. Met. Geomech.*, **37**(11), 1670-1684. https://doi.org/10.1002/nag.2159.

Burland, J.B., Longworth, T.I. and Moore, J.F.A. (1977), "A study of ground movement and progressive failure caused by a deep excavation in Oxford Clay", *Géotechnique*, **27**(4), 557-591. https://doi.org/10.1680/geot.1977.27.4.557.

Burland, J.B. (1989), "Ninth Laurits Bjerrum Memorial Lecture: "Small is beautiful"—the stiffness of soils at small strains", *Can. Geotech. J.*, **26**(4), 499-516. https://doi.org/10.1139/t89-064.

Brumund, W.F. and Leonards, G.A. (1973), "Experimental study of static and dynamic friction between sand and typical constuction materials", *J. Test. Eval.*, **1**(2), 162-165. https://doi.org/10.1520/JTE10893J.

Chai, J., Shen, S., Ding, W., Zhu, H. and Carter, J. (2014), "Numerical investigation of the failure of a building in Shanghai, China", *Comput. Geotech.*, **55**, 482-493. https://doi.org/10.1016/j.compgeo.2013.10.001.

Chowdhury, S.S., Deb, K. and Sengupta, A. (2016), "Effect of fines on behavior of braced excavation in sand: Experimental and numerical study", *Int. J. Geomech.*, **16**(1), 04015018, https://doi.org/10.1061/(ASCE)GM.1943-5622.0000487.

Dalgic, K.D., Hendriks, M.A. and Ilki, A. (2018), "Building response to tunnelling-and excavation-induced ground movements: using transfer functions to review the limiting tensile strain method", *Struct. Infrastruct. Eng.*, **14**(6), 766-779. https://doi.org/10.1080/15732479.2017.1360364.

DGJ08-11-2010 (2010), Foundation Design Code, Shanghai Housing and Urban-Rural Construction Management Committee; Shanghai, China.

Dong, Y., Burd, H. and Houlsby, G. (2016), "Finite-element analysis of a deep excavation case history", *Géotechnique*, **66**(1), 1-15 https://doi.org/10.1680/jgeot.14.P.234.

Finno, R.J. and Bryson, L.S. (2002), "Response of building adjacent to stiff excavation support system in soft clay", *J. Perform. Constr. Fac.*, **16**(1), 10-20. https://doi.org/10.1061/(ASCE)0887-3828(2002)16:1(10).

Finno, R.J., Lawrence, S.A., Allawh, N.F. and Harahap, I.S. (1991), "Analysis of performance of pile groups adjacent to deep excavation", *J. Geotech. Eng.*, **117**(6), 934-955. https://doi.org/10.1061/(ASCE)0733-9410(1991)117:6(934).

Goh, A.T.C., Teh, C.I. and Wong, K.S. (1997), "Analysis of piles subjected to embankment induced lateral soil movements", *J. Geotech. Geoenviron. Eng.*, **123**(9), 792-801. https://doi.org/10.1061/(ASCE)1090-0241(1997)123:9(792).

Goh, A.T.C., Wong, K.S., Teh, C.I. and Wen, D. (2003), "Pile response adjacent to braced excavation", *J. Geotech. Geoenviron. Eng.*, **129**(4), 383-386. https://doi.org/10.1061/(ASCE)1090-0241(2003)129:4(383).

Harahap, S.E. and Ou, C. (2020), "Finite element analysis of time-dependent behavior in deep excavations", *Comput. Geotech.*, **119**, 103300, https://doi.org/10.1016/j.compgeo.2019.103300.

Houhou, M.N., Emeriault, F. and Belounar, A. (2019), "Three-dimensional numerical back-analysis of a monitored deep excavation retained by strutted diaphragm walls", *Tunn. Undergr. Sp. Tech.*, **83**, 153-164. https://doi.org/10.1016/j.tust.2018.09.013.

Hsiao, E.C., Schuster, M., Juang, C.H. and Kung, G.T. (2012), "Reliability analysis and updating of excavation-induced ground settlement for building serviceability assessment", *J. Geotech. Geoenviron. Eng.*, **134**(10), 1448-1458. https://doi.org/10.1061/(ASCE)1090-0241(2008)134:10(1448).

Hsiung, B.C.B. (2019), "Observations of the ground and structural behaviours induced by a deep excavation in loose sands", *Acta Geotechnica*, **15**, 1577-1593. https://doi.org/10.1007/s11440-019-00864-0.

Huang, M., Zhang, C. and Li, Z. (2009), "A simplified analysis method for the influence of tunneling on grouped piles", *Tunn. Undergr. Sp. Tech.*, **24**(4), 410-422. https://doi.org/10.1016/j.tust.2008.11.005.

Jardine, R.J., Potts, D.M., Fourie, A.B. and Burland, J.B. (1986), "Studies of the influence of non-linear stress–strain characteristics in soil-structure interaction", *Géotechnique*, **36**(3), 377-396. https://doi.org/10.1680/geot.1986.36.3.377.

Kim, T. and Finno, R.J. (2012), "Effects of stress path rotation angle on small strain responses", *J. Geotech. Geoenviron. Eng.*, **138**(4), 526-534. https://doi.org/10.1061/(ASCE)GT.1943-5606.0000612.

Korff, M., Mair, R.J. and Van Tol, F.A.F. (2016), "Pile-soil interaction and settlement effects induced by deep excavations", *J. Geotech. Geoenviron. Eng.*, **142**(8), 04016034. https://doi.org/10.1061/(ASCE)GT.1943-5606.0001434.

Lee, C.I., Kim, E.K., Park, J.S. and Lee, Y.J. (2018), "Preliminary numerical analysis of controllable prestressed wale system for deep excavation", *Geomech. Eng.*, **15**(5), 1061-1070. https://doi.org/10.12989/gae.2018.15.5.1061.

Lam, S.Y., Ng, C.W.W. and Poulos, H.G. (2013), "Shielding piles from downdrag in consolidating ground", *J. Geotech. Geoenviron. Eng.*, **139**(6), 956-968. https://doi.org/10.1061/(ASCE)GT.1943-5606.0000764.

Liyanapathirana, D.S. and Nishanthan, R. (2016), "Influence of deep excavation induced ground movements on adjacent piles", *Tunn. Undergr. Sp. Tech.*, **52**, 168-181. https://doi.org/10.1016/j.tust.2015.11.019.

Loganathan, N., Poulos, H.G. and Xu, K. (2001), "Ground and pile-group responses due to tunnelling", *Soils Found.*, **41**(1), 57-67. https://doi.org/10.3208/sandf.41.57.

Leung, C.F., Lim, J.K., Shen, R.F. and Chow, Y.K. (2003), "Behavior of pile groups subject to excavation induced soil movement", *J. Geotech. Geoenviron. Eng.*,**129**(1), 58-65. https://doi.org/10.1061/(ASCE)1090-0241(2003)129:1(58).

Leung, Y.F., Soga, K., Lehane, B.M. and Klar, A. (2010), "Role of linear elasticity in pile group analysis and load test interpretation", *J. Geotech. Geoenviron. Eng.*, **136**(12), 1686-1694. https://doi.org/10.1061/(ASCE)GT.1943-5606.0000392.

Liang, R., Xia, T., Huang, M. and Lin, C. (2017), "Simplified analytical method for evaluating the effects of adjacent excavation on shield tunnel considering the shearing effect", *Comput. Geotech.*, **81**, 167-187. https://doi.org/10.1016/j.compgeo.2016.08.017.

Mansouri, H. and Asghari-Kaljahi, E. (2019), "Two dimensional finite element modeling of Tabriz metro underground station L2-S17 in the marly layers", *Geomech. Eng.*, **19**(4), 315-327. https://doi.org/10.12989/gae.2019.19.4.315.

Mu, L. and Huang, M. (2016), "Small strain based method for predicting three-dimensional soil displacements induced by braced excavation", *Tunn. Undergr. Sp. Tech.*, **52**, 12-22.

https://doi.org/10.1016/j.tust.2015.11.001.
Mu, L., Huang, M. and Finno, R.J. (2012), "Tunnelling effects on lateral behavior of pile rafts in layered soil", *Tunn. Undergr. Sp. Tech.*, **28**, 192-201. https://doi.org/10.1016/j.tust.2011.10.010.
Nam, K., Kim, J., Kwak, D., Rehman, H. and Yoo, H. (2020), "Structure damage estimation due to tunnel excavation based on indoor model test", *Geomech. Eng.*, **21**(2), 95-102. https://doi.org/10.12989/gae.2020.21.2.095.
Ng, C.W.W., Zheng, G., Ni, J. and Zhou, C. (2020), "Use of unsaturated small-strain soil stiffness to the design of wall deflection and ground movement adjacent to deep excavation", *Comput. Geotech.*, **119**, 103375. https://doi.org/10.1016/j.compgeo.2019.103375.
Ou, C., Liao, J. and Cheng, W. (2000), "Building response and ground movements induced by a deep excavation", *Géotechnique*, **50**(3), 209-220. https://doi.org/10.1680/geot.2000.50.3.209.
Pedro, A.M.G., Zdravković, L., Potts, D.M. and e Sousa, J.A. (2017), "Derivation of model parameters for numerical analysis of the Ivens shaft excavation", *Eng. Geol.*, **217**, 49-60. https://doi.org/10.1016/j.enggeo.2016.12.005.
Poulos, H.G. and Davis, E.H. (1980), *Pile Foundation Analysis and Design*, Wiley, New York, U.S.A.
Poulos H.G. (2001), "Piled raft foundations: Design and applications", *Géotechnique*, **51**(2), 95-113. https://doi.org/10.1680/geot.2001.51.2.95.
Prakoso, W.A. and Kulhawy, F.H. (2001), "Contribution to piled raft foundation design", *J. Geotech. Geoenviron. Eng.*, **127**(1), 17-24. https://doi.org/10.1061/(ASCE)1090-0241(2001)127:1(17).
Park K.H. (2004), "Elastic solution for tunneling-induced ground movements in clays", *Int. J. Geomech.*, **4**(4), 310-318. https://doi.org/10.1061/(ASCE)1532-3641(2004)4:4(310).
Pinto, F. and Whittle, A.J. (2014), "Ground movements due to shallow tunnels in soft ground. I: Analytical solutions", *J. Geotech. Geoenviron. Eng.*, **140**(4), 04013040. https://doi.org/10.1061/(ASCE)GT.1943-5606.0000948.
Potyondy, J.G. (1961), "Skin friction between various soils and construction materials", *Géotechnique*, **11**(4), 339-353. https://doi.org/10.1680/geot.1961.11.4.339.
Reul, O. and Randolph, M.F. (2003), "Piled rafts in overconsolidated clay: comparison of in situ measurements and numerical analyses", *Géotechnique*, **53**(3), 301-315. https://doi.org/10.1680/geot.2003.53.3.301.
Schuster, M., Kung, G.T.C., Juang, C.H. and Hashash, Y.M. (2009), "Simplified model for evaluating damage potential of buildings adjacent to a braced excavation", *J. Geotech. Geoenviron. Eng.*, **135**(12), 1823-1835. https://doi.org/10.1061/(ASCE)GT.1943-5606.0000161.
Shi, J., Wei, J., Ng, C.W.W. and Lu, H. (2019), "Stress transfer mechanisms and settlement of a floating pile due to adjacent multi-propped deep excavation in dry sand", *Comput. Geotech.*, **116**, 103216, https://doi.org/10.1016/j.compgeo.2019.103216.
Skempton, A.W. and MacDonald, D.H. (1956), "The allowable settlements of buildings", *Proc. Inst. Civ. Eng.*, **5**(6), 727-768. https://doi.org/10.1680/ipeds.1956.12202.
Soomro, M.A., Mangnejo, D.A., Bhanbhro, R., Memon, N.A. and Memon, M.A. (2019), "3D finite element analysis of pile responses to adjacent excavation in soft clay: Effects of different excavation depths systems relative to a floating pile", *Tunn. Undergr. Sp. Tech.*, **86**, 138-155. https://doi.org/10.1016/j.tust.2019.01.012.
Sinha, A. and Hanna, A.M. (2017), "3D numerical model for piled raft foundation", *Int. J. Geomech.*, **17**(2), 04016055. https://doi.org/10.1061/(ASCE)GM.1943-5622.0000674.
Whittle, A.J., Hashash, Y.M. and Whitman, R.V. (1993), "Analysis of deep excavation in Boston", *J. Geotech. Eng.*, **119**(1), 69-90. https://doi.org/10.1061/(ASCE)0733-9410(1993)119:1(69).
Wroth, C. and Burland, J.B. (1974), "Settlement of buildings and associated damage", *Proceedings of the British Geotechnical Society's Conference on Settlement of Structures*, Cambridge, U.K., April
Xu, K. and Poulos, H.G. (2001), "3-D elastic analysis of vertical piles subjected to "passive" loadings", *Comput. Geotech.*, **28**(5), 349-375. https://doi.org/10.1016/S0266-352X(00)00024-0.
Zheng, G., Du, Y., Cheng, X., Diao, Y., Deng, X. and Wang, F. (2017), "Characteristics and prediction methods for tunnel deformations induced by excavations", *Geomech. Eng.*, **12**(3), 361-397. https://doi.org/10.12989/gae.2017.12.3.361.

CC